SEGMENTED CAPACITANCE SENSOR WITH PARTIALLY RELEASED INACTIVE SEGMENTS*

J. Lev, V. Prošek, P. Novák, F. Kumhála, M. Wohlmuthová

Czech University of Life Sciences Prague, Faculty of Engineering, Prague, Czech Republic

Material throughput measurement is important for many applications, for example yield maps creation or control of mass flow in stationary lines. Quite perspective can be the capacitive throughput method. Segmented capacitance sensor (SCS) is discussed in this paper. SCS is a compromise between simple capacitive throughput sensors and electrical capacitance tomography sensors. The SCS variant with partially released inactive segments is presented. The mathematical model of SCS was created and verified by measurements. A good correspondence between measured and computed values was found and it can be stated that the proposed mathematical model was verified. During measurement the voltage values on the inactive segments were monitored as well. On the basis of the measurement there was found that these values are significantly influenced by material distribution.

finite element method; throughput; electrical capacitance tomography; mathematical model

DE GRUYTER OPEN

doi: 10.1515/sab-2015-0022

Received for publication on April 16, 2014

Accepted for publication on February 26, 2015

INTRODUCTION

Material throughput measurement is used in many agriculture and industry applications. One possibility of throughput measurement can be the capacitive throughput sensor according to Stafford et al. (1996) and Savoie et al. (2002). The authors presented the advantages as: non-contact measurement, simple mounting on the machine, simplicity of the sensor, and low cost.

The capacitive throughput sensor was developed at the Department of Agriculture Machines of the Czech University of Life Sciences Prague. This sensor was tested for throughput measurement of forage material, sugar beets, potatoes, and hops (Kumhála et al., 2007, 2009, 2013).

Kumhála et al. (2009) described the filling theory of the capacitive throughput sensor. It is very important that capacity of sensor depends on the distribution of material between its plates. Nevertheless, the simple capacitive throughput sensors cannot provide information about material distribution. This fact can produce significant errors. This problem can be resolved with an electrical capacitance tomography (ECT). The principle of ECT is based on the multiple capacitance measurement of the sensing area. In this place there are typically two materials and each has different dielectric properties. On the basis of capacitance measurements the distribution of materials is determined. The ECT sensors were tested for: determining of solid particles distribution in the air flow (Williams, Xie, 1993), determining of oil and gas distribution in the oil pipeline (Gamio, 2002), monitoring of burning fuel in a combustion engine (Waterfall et al., 1996), or monitoring of material distribution on the conveyor belt (Williams et al., 2000).

Usually ECT sensors are composed of 8–14 electrodes. This means that 28–120 independent capacitance measurements are obtained. The problem is that capacitance changes are very small and they have to be measured in a large range. For example Yang (2010) presents values of capacitance change between 0.1 fF to 0.1 pF. This author also suggests that measurement accuracy should be about 0.01 fF and better. It is evident that ETC sensors are very complicated devices and for some applications (throughput measurement) a simpler device can be used. An interesting possibility can be the segmented capacitance sensor (SCS).

* Supported by the Internal Grant Agency of the Faculty of Engineering, Czech University of Life Sciences Prague (Project No. 2013:31160/1312/3114).

The idea of SCS has already been described in several papers (Kumhála et al., 2012; Lev et al., 2013a). The important parts are two plates between which a measured material can flow. The bottom plate is undivided while the upper plate is divided into several segments in order to obtain several measurements. This is a fundamental difference from ECT sensors, which usually produce much more output signals. It is thus necessary to use a different approach towards the solution of the inverse problem. For developing of the SCS the mathematical model is very important. The mathematical model is useful for algorithm solving inverse problem development and also for its design optimization.

For obtaining a mathematical model a standard way which is known from ECT can be used. However, in this case there is a problem with measurement segments which are currently not used for measurement. These segments are called inactive segments. In another study (Lev et al., 2013a) these segments were completely insulated from the measurement circuit and from the grounded parts of sensor. These segments were labelled as "released segments". Although released segments were not used directly for measurement, the effect was significant due to floating potentials in the areas of segments. As for the image reconstruction, it is desirable to have a reliable mathematical model of an electric field, and it is necessary to calculate the values of floating potential with sufficient accuracy. This can be problematic, because the values of floating potentials can be affected by parasitic capacitances in real conditions. These parasitic capacitances are typically made up of a switch that connects and disconnects the segment to the measurement circuit.

One of the ways to work around this problem is connection of the inactive segments to the ground terminal. In the mathematical model the domains of segments will be removed and on their edges Dirichlet boundary conditions will be defined. This step simplifies the mathematical model but certainly also reduces the sensitivity of the sensor (Lev et al., 2013b).

In this paper another possibility is discussed. For each segment the simple measurement circuit is connected. Using this circuit the potential on the inactive segments is determined. In the mathematical model the domains of segments are removed and on their edges Dirichlet boundary conditions from measured values are defined.

MATERIAL AND METHODS

For the purpose of this work a simple SCS prototype was made (see the scheme in Fig. 1). The frame was made from phenolic paper sheet plate (Hp 2061) and each plate was 10 mm thick. Important is the size of the sensing area which is 100 × 400 mm. The depth of the sensing area is 400 mm. All electrodes are made of a 1-mm-thick copper sheet. The size of the bottom electrode (bottom plate) is the same as the bottom part of the sensing area, i.e. 400 × 400 mm. The sensor has 8 measuring segments each 400 mm in length and 40 mm in width. Another part is the grounded steel cage which is used for shielding in order to remove the influence of surrounding effects. The size of the cage is 1000 mm in width and 500 mm in height.

The connection of the measuring circuit is shown in Fig. 2. For measuring of small capacitance changes the measuring circuit based on the divider circuit was used. This circuit was described in details by Kumhála et al. (2007). The circuit to the fourth and fifth measuring segment was connected and these segments were labelled as 'active segments'. The other segments were not used during measurement and they were labelled as 'inactive segments'. To each segment a simple measuring circuit was connected. The circuit consists of an AC/DC rectifying module and voltmeter.

For the purpose of SCS behaviour testing measurement was proposed. The test sample in the sensing area was being moved and the sensor responses were monitored. Two types of testing samples were used during measurement. Both test samples were 300 mm in length and 50 mm in width and only the height was different. Material of the test samples was the same as the frame of SCS. The height of the first test sample

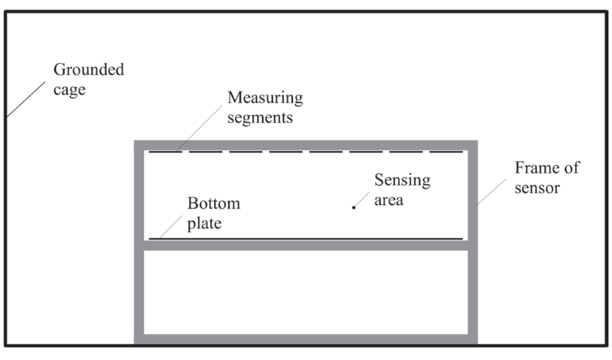

Fig. 1. Scheme of the segmented capacitance sensor without the measuring circuit

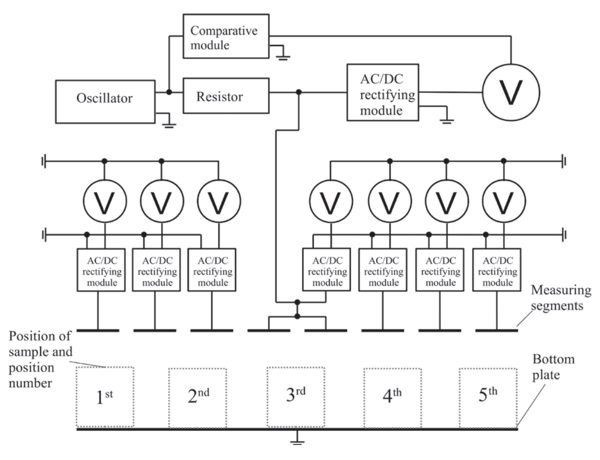

Fig. 2. Connection of the measuring circuit to the segmented capacitance sensor during experiments

was 40 mm, while of the second one it was 80 mm. In both cases, the sample was placed on five positions. The positions of the sample are specified in Fig. 2. The 1st and 5th positions were on the borders of the sensing area. The 3rd position was exactly in the centre of the sensing area and the 2nd and 4th positions were in the centre between the 1st and the 3rd or the 3rd and the 5th position, respectively.

The outputs of the measurements were voltage changes due to the test sample which was placed on the position in the sensing area. The voltage change was the difference between a situation when the sensor was empty and when the test sample was in the sensing area. The measurement for each position and with both samples was performed and repeated five times. During each of the measurements, the voltages from the simple measuring circuits were also recorded. Thus, during each of the measurements, one voltage value was obtained from the main circuit and the other seven were obtained from auxiliary circuits.

The most important part of this work is the mathematical model of segmented capacitance sensor. According to numerous studies (e.g. Xie et al., 1992; Williams, Beck, 1995; Yang, Liu, 1999; Lev et al., 2013a) the following equation was used for electric field description:

$$\nabla \cdot (\varepsilon \nabla \varphi) = 0 \tag{1}$$

where:
∇ = nabla operator
φ = electric scalar potential (V)
$\varepsilon = \varepsilon_0\, \varepsilon_r$ ($\varepsilon_0 = 8.854 \times 10^{-12}$ (F m^{-1}) and ε_r = relative permittivity (–))

In this model only two types of materials (air and phenolic paper sheet) were used. Relative permittivity of the air was $\varepsilon_r = 1$ but for phenolic paper sheet two variants of relative permittivity were performed ($\varepsilon_r = 4.5$ and 5) because the influence of relative permittivity was tested as well.

Equation (1) was resolved by the finite element method using Agros2D 3.0 software. This software is able to work with a higher-order finite element method with hp-adaptivity based on reference solution and local projections (Karban et al., 2013). The described method has been well applicable to our problem solution. All boundary conditions were defined as Dirichlet conditions. For the elements which were connected to the grounding conductor (the bottom electrode and cage) the boundary conditions were $\varphi_\Gamma = 0$ V. The boundary conditions on the measuring segments on the based measured values were defined.

To calculate the impedance of the sensor the following equation was used:

$$Z = \frac{U}{I} \tag{2}$$

where:
Z = impedance of the sensor (Ω)
U = difference between electric potential on the active segments and electric potential on the grounding parts of the sensor (V)
I = current which passes through the active segments (A)

The current can be calculated from equation

$$I = 2\pi f \int_\Gamma \varepsilon E \cdot d\Gamma \tag{3}$$

where:
π = Ludolph's number
f = frequency (Hz)
E = vector of electric field intensity (V.m^{-1})
$d\Gamma$ = normal vector of the area element
Γ = electrode surface (m^2)

RESULTS

The calculated impedance changes and measured voltage changes cannot be directly compared. It is necessary to recalculate the values on the relative changes for this purpose. For the voltage changes the following equation can be used:

$$U_r = \frac{\Delta U}{\Delta U_{100}} 100 \tag{4}$$

where:
U_r = relative voltage change (%)
ΔU = measuring voltage change (V)
ΔU_{100} = reference voltage change (V) caused by the sample in the reference position (3rd)

A similar equation can be used for calculating a relative impedance change:

$$Z_r = \frac{Z_0 - Z}{Z_0 - Z_{100}} 100 \tag{5}$$

where:
Z_r = relative impedance change (%)
Z_0 = impedance of the empty sensor (Ω)
Z = calculated impedance (Ω) using Eqs (2) and (3)
Z_{100} = calculated impedance (Ω) caused by the sample in the reference position

The comparison of the measured and computed values is given in Fig. 3. Graphs (a) and (b) show a situation where the test sample was 40 mm and 80 mm high, respectively. The black dashed curves show computed values and the grey curve shows measured values.

The main goal of this work was the mathematical model of SCS creation and its verification. In Fig. 3 it can be seen that the computed and measured values are quite well corresponding. There are only small differences which may be caused by geometric imperfections and inaccuracy of the numerical solution. Stability of the measuring circuit was tested as well. The estimates of the relative measuring error ranged up to 3% (significance level $\alpha = 0.05$).

Table 1. Average voltage values (V) on the measuring segments obtained during measurement

Sample height (mm)	Sample position	Number of segment							
		1st	2nd	3rd	4th	5th	6th	7th	8th
40	1st	0.52	0.83	1.47	2.93	2.93	1.47	0.80	0.51
	2nd	0.52	0.81	1.44	2.93	2.93	1.47	0.80	0.51
	3rd	0.53	0.83	1.45	2.89	2.89	1.44	0.78	0.50
	4th	0.54	0.84	1.47	2.92	2.92	1.44	0.77	0.48
	5th	0.54	0.84	1.48	2.93	2.93	1.46	0.79	0.48
80	1st	0.47	0.80	1.46	2.93	2.93	1.47	0.80	0.51
	2nd	0.49	0.76	1.35	2.89	2.89	1.45	0.79	0.50
	3rd	0.50	0.79	1.38	2.77	2.77	1.38	0.75	0.48
	4th	0.53	0.83	1.45	2.89	2.89	1.35	0.72	0.46
	5th	0.54	0.84	1.48	2.93	2.93	1.45	0.76	0.45
Empty sensor		0.54	0.85	1.48	2.93	2.93	1.47	0.80	0.51

In Table 1 there are voltage values which were obtained from auxiliary circuits. Each voltage value is an average from five measured values. Estimates of the relative measuring error did not exceed 3% (significance level $\alpha = 0.05$).

DISCUSSION

The first important result of the comparison in Fig. 3 is that there is no significant difference between the calculation with relative permittivity $\varepsilon_r = 4.5$ and calculation with relative permittivity $\varepsilon_r = 5$ (dash and dot lines). It means that the mathematical model is not much sensitive to the wrongly determined relative permittivity of sensor frame material. The reason is that for forming of an electric field in the sensing area the electric potential values on the segments are the most important. These values are directly determined by measurement and they are not calculated during solving of Eq. (1).

Fig. 3 shows that differences between calculated and measured values are quite small and it can be stated that calculations correspond with measurement. Greater differences were found during the measurement with the smaller sample. It may be caused by approximately four times smaller circuit sensitivity in this case. Voltage changes for the smaller test sample were up to 99 mV and voltage changes for the bigger test sample were up to 390 mV. In these cases the measured errors can have a more significant influence.

The important information is that not only the voltage on the 4th and 5th segment was changed due to moving the test sample (here the main measuring circuit was connected), but the voltages on the inactive segments were changed as well. Quite interesting is the fact that relative voltage changes on the inactive segments are greater than on the active segments. This behaviour can be useful because it means that this arrangement of SCS is able to produce more output signals which can be used for better image reconstruction. However, voltage changes on the inactive seg-

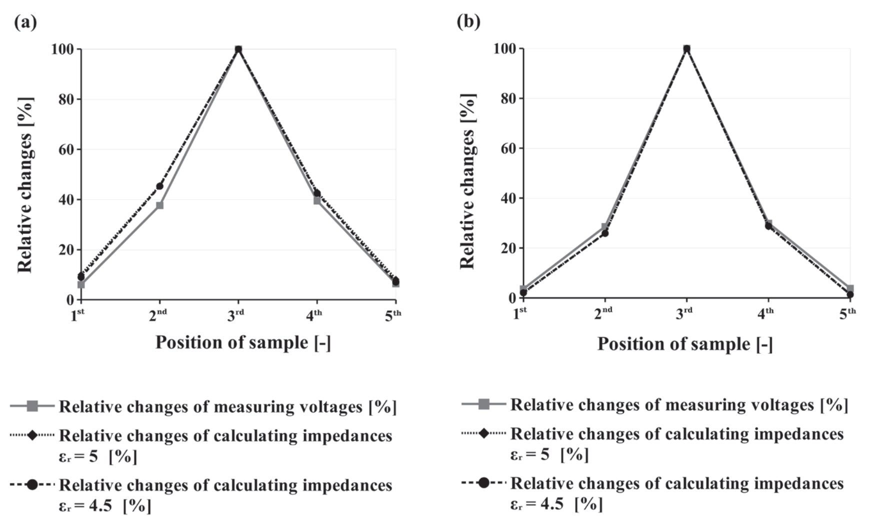

Fig. 3. Comparison of measured and computed values. Measurement and calculation with a test sample (a) 40 mm in height, (b) 80 mm in height

ments caused by the change of material distribution in the sensing area would be hardly estimable just on the theoretical basis, without measurement.

CONCLUSION

In this paper the SCS with partially released inactive segments was tested. The main objective was to propose and verify a mathematical model. The measured and computed values of the proposed mathematical model were found to be well corresponding and its verification can thus be stated. During the measurement it was found out that voltage values on the inactive segments were significantly influenced by the test sample position in the sensing area. It means that this arrangement of SCS is able to produce more output signals which can be used for better image reconstruction. However, the research should continue in the outlined direction because the determination of voltage values on the inactive segments without measurement was not resolved within the current study.

REFERENCES

Gamio JC (2002): A comparative analysis of single and multiple-electrode excitation methods in electrical capacitance tomography. Measurement Science and Technology, 13, 1799–1809. doi: 10.1088/0957-0233/13/12/301.

Karban P, Mach F, Kůs P, Pánek D, Doležel I (2013): Numerical solution of coupled problems using code Agros2D. Computing, 95 (Suppl. 1), 381–408. doi: 10.1007/s00607-013-0294-4.

Kumhála F, Kvíz Z, Kmoch J, Prošek V (2007): Dynamic laboratory measurement with dielectric sensor for forage mass flow determination. Research in Agricultural Engineering, 53, 149–154.

Kumhála F, Prošek V, Blahovec J (2009): Capacitive throughput sensor for sugar beets and potatoes. Biosystems Engineering, 102, 36–43. doi: 10.1016/j.biosystemseng.2008.10.002.

Kumhála F, Lev J, Wohlmuthová M, Prošek V (2012): First tests with segmented capacitive throughput sensor. Scientia Agriculturae Bohemica, 43, 1, 22–27.

Kumhála F, Kavka M, Prošek V (2013): Capacitive throughput unit applied to stationary hop picking machine. Computers and Electronics in Agriculture, 95, 92–97. doi: 10.1016/j.compag.2013.04.012.

Lev J, Mayer P, Wohlmuthová M, Prošek V (2013a): The mathematical model of experimental sensor for material distribution detecting on the conveyor. Computing, 95 (Suppl. 1), 521–536. doi: 10.1007/s00607-012-0273-1.

Lev J, Prošek V, Wohlmuthová M, Kumhála F (2013b): The mathematical model of segmented capacitance sensor with grounded segments for determining of material distribution on the conveyor. Agronomy Research, 11, 73–80.

Savoie P, Lemire P, Thériault R (2002): Evaluation of five sensors to estimate mass-flow rate and moisture of grass in a forage harvester. Applied Engineering in Agriculture, 18, 389–397.

Stafford JV, Ambler B, Lark RM, Catt J (1996): Mapping and interpreting the yield variation in cereal crops. Computers and Electronics in Agriculture, 14, 101–119. doi: 10.1016/0168-1699(95)00042-9.

Waterfall RC, He R, White NB, Beck CB (1996): Combustion imaging from electrical impedance measurements. Measurement Science and Technology, 7, 369–374. doi: 10.1088/0957-0233/7/3/018.

Williams RA, Xie CG (1993): Tomographic techniques for characterizing particulate process. Particle & Particle Systems Characterization, 10, 252–261. doi: 10.1002/ppsc.19930100507.

Williams RA, Beck MS (eds) (1995): Process tomography, principles, techniques and applications. Butterworth-Heinemann, Oxford.

Williams RA, Luke SP, Ostrowski KL, Bennett MA (2000): Measurement of bulk particulates on belt conveyor using dielectric tomography. Chemical Engineering Journal, 77, 1–2, 57–63. doi: 10.1016/S1385-8947(99)00146-1.

Xie CG, Huang SM, Hoyle BS, Thorn R, Lenn C, Snowden D, Beck MS (1992): Electrical capacitance tomography for flow imaging system model for development of image reconstruction algorithms and design of primary sensors. Circuits, Devices and Systems, IEE Proceedings G, 139, 89–98.

Yang WQ (2010): Design of electrical capacitance tomography sensors. Measurement Science and Technology, 21, 1–13. doi: 10.1088/0957-0233/21/4/042001.

Yang WQ, Liu S (1999): Electrical capacitance tomography with a square sensor. In: Proc. 1st World Congress on Industrial Process Tomography, Buxton, Greater Manchester, 313–317.

Corresponding Author:

Ing. Jakub L e v , Ph.D., Czech University of Life Sciences Prague, Faculty of Engineering, Department of Physics, Kamýcká 129, 165 21 Prague 6-Suchdol, phone: +420 224 383 281, e-mail: jlev@tf.czu.cz